

Supplementary Information for

A Spatiotemporally Defined *In-Vitro* Microenvironment for Controllable Signal Delivery and Drug Screening

Ching-Te Kuo^{a,b*}, Hao-Kai Liu^{a*}, Guan-Syuan Huang^a, Chi-Hao Chang^c, Chen-Lin Chen^a,
Ken-Chao Chen^a, Ruby Yun-Ju Huang^{d,e}, Ching-Hung Lin^f, Hsinyu Lee^{c**},
Chiun-Sheng Huang^{g**}, and Andrew M. Wo^{a**}

^a*Institute of Applied Mechanics, National Taiwan University, Taipei, Taiwan, R.O.C.*

^b*Institute of Atomic and Molecular Sciences, Academia Sinica, Taipei, Taiwan, R.O.C.*

^c*Department of Life Science, National Taiwan University, Taipei, Taiwan, R.O.C.*

^d*Department of Obstetrics & Gynaecology, National University Hospital, Singapore*

^e*Cancer Science Institute of Singapore, National University of Singapore, Singapore*

^f*Department of Oncology, National Taiwan University Hospital, Taipei, Taiwan, R.O.C.*

^g*Department of Surgery, National Taiwan University Hospital, Taipei, Taiwan, R.O.C.*

* These authors contributed equally to this work

** Prof. Hsinyu Lee. E-mail: hsinyu@ntu.edu.tw or

** Prof. Chiun-Sheng Huang. E-mail: huangcs@ntu.edu.tw or

** Prof. Andrew M. Wo. E-mail: andrew@iam.ntu.edu.tw

Supplementary information file includes 1 tables, 4 figures, and 1 references.

Evaluation of the evaporation-driven velocity

100 μl medium was first individually loaded to all solution wells in the microfluidic device, followed by placing the device in the incubator at 37°C for one day. Four experimental sets were conducted by inserting different types of customized papers (type 1 ~ type 4 in Table S1) to the outlet wells (wells T2 and T4), to create a particular pumping velocity driven by the differentiated evaporation rates. Table S1 shows the detailed specifics of the customized papers used in this work. This experiment was conducted with no cells. After one-day culturing, we measured the mass of residual medium in the wells, and the changed mass M_{ave} was then calculated as that the residual mass from type 1 set (that is, without paper inserting as a control set) subtracts the one from the particular types, suggesting that the differentiated mass could be corresponding to the differentiated evaporation rate and the resulting pumping flow (Fig. 2a). We assumed that the density of medium is equivalent to DI water, that is, 1 g/cm^3 ; therefore, the corresponding average volume changed U_{ave} (μl) is equivalent to M_{ave} (mg). The following driven velocity was evaluated as $(U_{ave} / \text{day}) / A_{channel}$, where $A_{channel}$ is the cross-sectional area of the top channel and $A_{channel} = 54000 \mu\text{m}^2$.

Simulation of concentration gradient developed in the microfluidic device

To assess the concentration gradient of dextran within the device, a commercial finite-element package (COMSOL 4.2) was utilized to simulate and analyze the gradient (Fig. S1). Initial concentration boundary conditions were defined at the condition channel with 50 ng/ml and sink conditions at the cell channel. The diffusion coefficient of $3 \sim 5 \text{ kDa}$ dextran in scaffolds (1 mg/ml) was assumed to be $12.3 \times 10^{-11} \text{ m}^2/\text{s}$, based on a scaling law for soluble factors diffusing in free solutions. In 2.5 mg/ml collagen scaffolds, the comparison ($D_{scaffold} / D_{solution} \sim 0.94$) is very similar,¹ suggesting that this assumption could be applied in our simulation. Figs. S1 b and c show the quantification results of the simulated concentration profile, indicating that a uniform gradient of 25.2 ng/ml/mm could be performed by this approach.

Quantified cell migration

Fig. S3 shows the method used to measure the number and distance/velocity of cell migration. For the proof-of-concept, we herein detected the cell nucleus as the tracking

point. To determine the time-dependent process, EGF was loaded in the condition channel for 1 ~ 4 days after cells/spheroids seeding. Images of cell migration were taken daily and processed off-line by Image J software to track cells. For each cell tracking, the following measurements were made: the radius of cell trapping region r_1 ($r_1 = 75 \mu\text{m}$), the distance travelled r_2 , and the oriented angle θ . Cells were considered migratory while they travelled over the cell trapping region, thus the net distance travelled d can be defined as $d = r_2 - r_1$. The average migration velocity per cell was then estimated as $\sum_m (d_n - d_{n-1})_m / m_{total} / \text{Day}_n$, where m (≥ 1) and n (≥ 1) indicates the cell number and the specific day, respectively, and m_{total} represents the total cell number. In our case, it was complicated to precisely track the migratory cells from Day 0 to Day 1 due to that the original location of these cells within the tumor spheroids at Day 0 was poorly distinguishable. Therefore, the average migration velocity was only determined from Day 2 to Day 4 except for Day 1 in this work (Figs. 3c and 3d). In addition, the migration distance d described above may be applicable due to the migratory paths of cells were straightforward following the migratory pattern shown in Fig. 3a.

Supplementary Table

Table S1. The specifics of the customized papers

Paper type	Type 1	Type 2	Type 3	Type 4
Exposed area (A ; mm ²)	0.00	52.32	104.16	136.71
Changed mass (M_{ave} /day; mg/day)	0.00	34.10 ± 14.97	54.25 ± 8.53	93.15 ± 9.56
Changed volume (U_{ave} /day; μl/day)	0.00	34.10 ± 14.97	54.25 ± 8.53	93.15 ± 9.56
Driven velocity (V_d ; μm/s)	0.00	7.31 ± 3.21	11.63 ± 1.83	19.97 ± 2.05
Péclet number ($Pe = UI/D$; U is the driven velocity, l is the characteristic length, and D is the molecular diffusivity)	0.00	59.43	94.55	162.36

Supplementary Figures

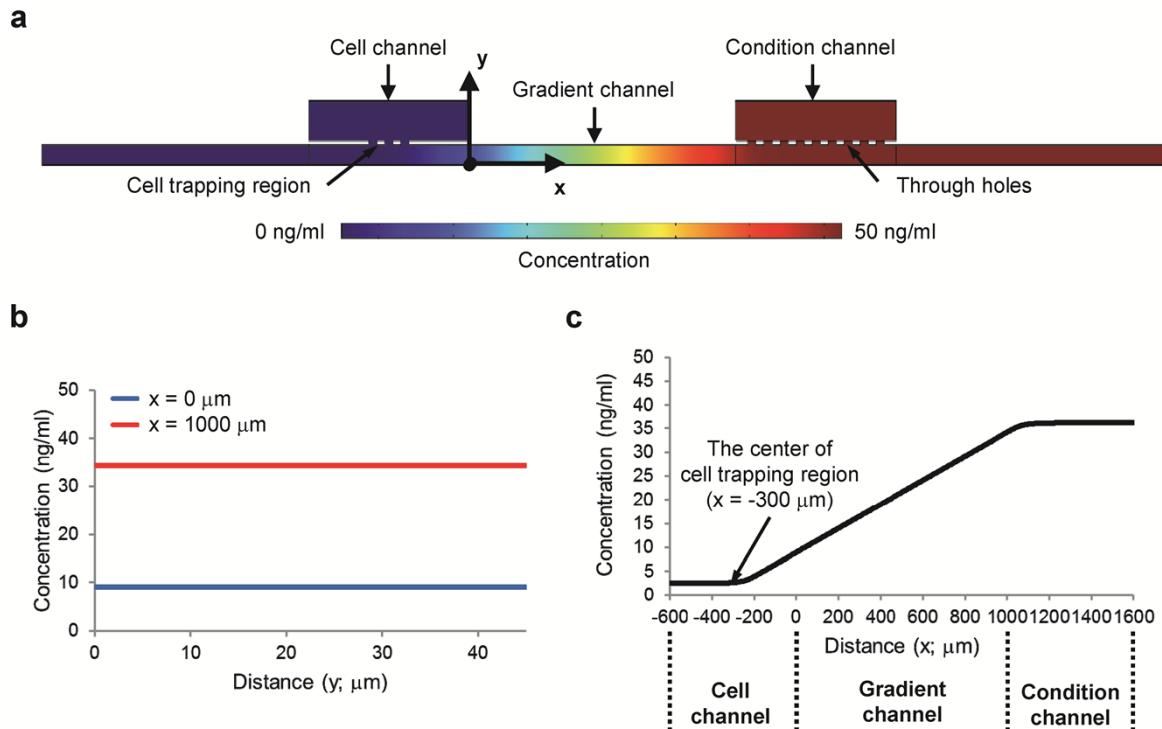


Figure S1. Numerical simulations of dextran concentration distributed in the microfluidic device. (a) shows the cross-sectional view of the simulated device, including two top channels (one is indicated as cell channel and the other is indicated as condition channel) and one bottom channel as gradient channel. Results show that uniform concentration profiles were performed along the y-axis direction at $x = 0 \mu\text{m}$ and $x = 1000 \mu\text{m}$, respectively, in the gradient channel (b), and a stable gradient of 25.2 ng/ml/mm was performed along the x-axis direction in the gradient channel (c). Based on the simulation, the actual concentration on tumor spheroid in the cell culture region is assumed to be multiplied by 6.8%, corresponding to the initial concentration C_0 applied.

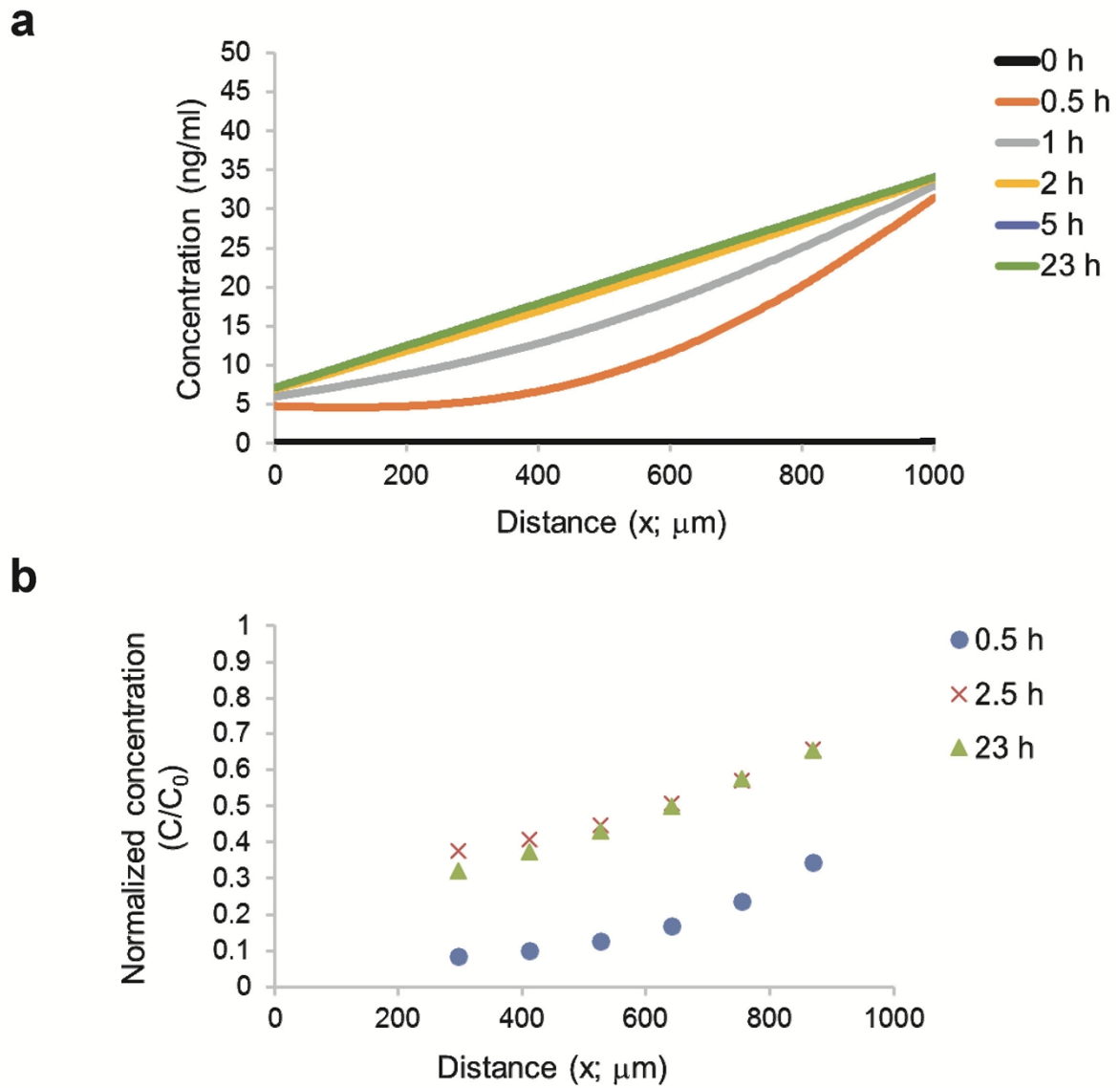


Figure S2. Time domain responses of the concentration profile distributed in the microdevice. (a) shows the time-sequenced simulations of concentration gradient from Figure S1. (b) shows the experimental measurements of concentration gradient at time = 0.5 h, 2.5 h, and 23 h. These results indicate that the time taken to stabilize the gradient is around two hours in this work.

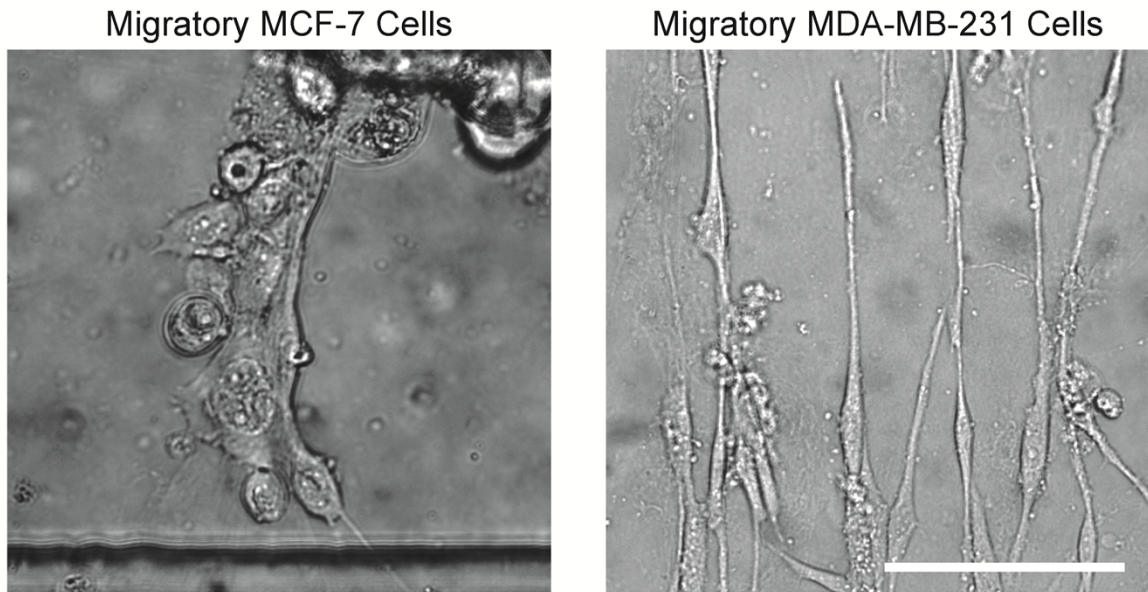


Figure S3. Two different migrator patterns of cancer cells. The left image shows the migratory MCF-7 cells and the right one shows the migratory MDA-MB-231 cells. Scale bar: 100 μm .

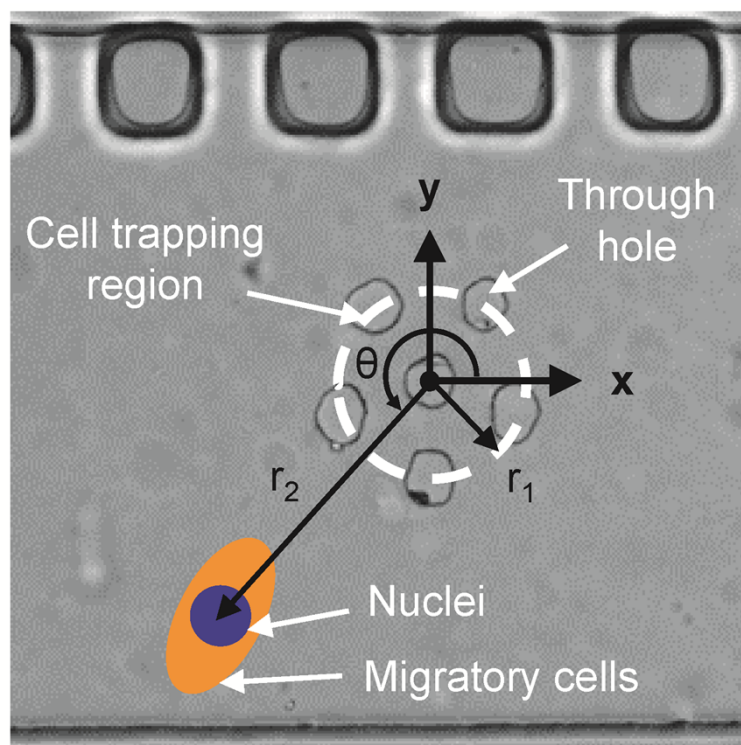


Figure S4. Schematic measurement on migratory cell number and migration distance/velocity.

Reference

1. I. K. Zervantonakis, S. K. Hughes-Alford, J. L. Charest, J. S. Condeelis, F. B. Gertler and R. D. Kamm, *Proc. Natl. Acad. Sci. U. S. A.*, 2012, **109**, 13515-13520.